Title

Individual Differences in Adult Reading Are Associated with Left Temporo-parietal to Dorsal Striatal Functional Connectivity

Journal

Cerebral Cortex, 26(10)

ISSN

1047-3211

Authors

Achal, Sanjay
Hoeft, Fumiko
Bray, Signe

Publication Date

2016-10-01

DOI

10.1093/cercor/bhv214

Peer reviewed

Cerebral Cortex, October 2016;26: 4069–4081

doi:10.1093/cercor/bhv214
Advance Access Publication Date: 22 September 2015
Original Article

ORIGINAL ARTICLE

Individual Differences in Adult Reading Are Associated with Left Temporo-parietal to Dorsal Striatal Functional Connectivity

Sanjay Achal[1,2], Fumiko Hoeft[4,5,6], and Signe Bray[3,7,8,9]

[1]Department of Neuroscience, [2]Hotchkiss Brain Institute, [3]Department of Radiology, University of Calgary, Calgary, AB, Canada T2N 4N1, [4]Division of Child and Adolescent Psychiatry, Department of Psychiatry, University of California, San Francisco, CA 94143, USA, [5]Haskins Laboratories, Yale University, New Haven, CT 06511, USA, [6]Department of Neuropsychiatry, Keio University School of Medicine, Tokyo 160-8582, Japan, [7]Department of Paediatrics, [8]Alberta Children's Hospital Research Institute and [9]Child and Adolescent Imaging Research Program, Alberta Children's Hospital, Calgary, AB, Canada T3B 6A8

Address correspondence to Signe Bray, 2888 Shaganappi Trail NW, Calgary, AB, Canada T3B 6A8. Email: slbray@ucalgary.ca; Fumiko Hoeft, 401 Parnassus Avenue, Box 0984-F, San Francisco, CA 94143, USA. Email: fumiko.hoeft@ucsf.edu

Abstract

Reading skills vary widely in both children and adults, with a number of factors contributing to this variability. The most prominent factor may be related to efficiency of storage, representation, or retrieval of speech sounds. This phonological hypothesis is supported by findings of reduced activation in poor readers in left hemisphere ventro-lateral prefrontal and temporo-parietal phonological processing regions. Less well explained by phonological theories are reported hyperactivation in prefrontal, striatal, and insular regions. This study investigated functional connectivity of a core phonological processing region, the temporo-parietal junction (TPJ), in relation to reading skill in an adult community sample. We hypothesized that connectivity between TPJ and regions implicated in meta-analyses of reading disorder would correlate with individual differences in reading. Forty-four adults aged 30–54, ranging in reading ability, underwent resting fMRI scans. Data-driven connectivity clustering was used to identify TPJ subregions for seed-based connectivity analyses. Correlations were assessed between TPJ connectivity and timed-pseudoword reading (decoding) ability. We found a significant correlation wherein greater left supramarginal gyrus to anterior caudate connectivity was associated with weaker decoding. This suggests that hyperactivation of the dorsal striatum, reported in poor readers during reading tasks, may reflect compensatory or inefficient overintegration into attention networks.

Key words: caudate, functional connectivity, reading, temporo-parietal junction

Introduction

Fluent reading depends on efficient integration and binding of phonological, lexical, and semantic information. Despite the ubiquity of reading in modern society, reading competence varies widely in the population, with dyslexia or specific reading disorder (RD) identified in the lower tail of a continuous normal distribution (Shaywitz et al. 1992).

A number of factors have been linked to interindividual variability in reading competence and RD including variability in attention (Facoetti et al. 2000) and processing speed (Bogon et al. 2014). However, the most prominent contributor may be variability in the ability to represent, store, or retrieve speech sounds (Bradley and Bryant 1978; Wagner and Torgesen 1987; Snowling 1998). Phonological processing relies heavily on left

hemisphere temporo-parietal language and auditory regions (Vigneau et al. 2006). Meta-analyses of reading-relevant functional and neuroanatomical correlates of RD (Maisog et al. 2008; Richlan et al. 2009, 2011, 2013; Linkersdörfer et al. 2012), as well as studies of interindividual variability in reading competence (Koyama et al. 2011), highlight the role of regions including the temporo-parietal junction (TPJ).

The TPJ is a region at the intersection of the posterior temporal sulcus, inferior parietal lobule, and lateral occipital cortex that has been implicated in several theories of RD. The left TPJ is thought to play a role in the encoding and retrieval of speech sounds (Ravizza et al. 2004), and abnormal connectivity of this region has been hypothesized to specifically relate to difficulties in retrieval of speech sounds during reading (Boets et al. 2013). Another theory of RD posits dysfunction in the magnocellular system as part of the dorsal visual processing stream (Demb et al. 1998). The dorsal visual processing stream has been argued to contain dorsal and ventral subdivisions, where the dorsal portion (d-d) includes the intraparietal sulcus and the ventral portion (v-d) includes inferior parietal regions encompassed by the TPJ (Rizzolatti and Matelli 2003); abnormal connectivity along this pathway may relate to visuospatial and visual processing deficits seen in RD (Demb et al. 1998; Franceschini et al. 2012). Portions of the TPJ are structurally and functionally connected to the dorsal attention network. Reading difficulties may also stem from the lack of a functionally distinct attention network (Koyama et al. 2013) or impaired TPJ-mediated attentional processes (Ravizza et al. 2011). Finally, the TPJ has been implicated in cerebellar theories of RD: the cerebellum is important during silent reading and language comprehension to help detect errors, direct attention, and ensure proper timing/sequencing (Fabbro 2000). Imaging studies have suggested that the cerebellum is a key part of a normative reading network and is actively connected to the right TPJ during reading (Turkeltaub et al. 2003).

Thus, several theories of RD implicate the TPJ through different functional networks: language, attentional, visual, and cerebellar. This is notable in light of the fact that the TPJ is located at the intersection of several brain networks (Mars et al. 2012; Bzdok et al. 2013; Power et al. 2013; Bray et al. 2015). Examining the relationship between functional connectivity and reading measures within each of these subnetworks may shed light on the neural mechanisms underlying interindividual variability in reading competence.

In addition to functional and structural correlates of reading around the TPJ that generally show decreased activation and gray matter in individuals with RD (Hoeft et al. 2007; Linkersdörfer et al. 2012; Krafnick et al. 2014), there have been consistent findings of increased activation in frontal, thalamic, dorsal striatal, and insular regions in individuals with RD (Maisog et al. 2008; Richlan et al. 2009, 2011; Diehl et al. 2014). Increased activation in less skilled readers has been attributed to overengagement, due to increased difficulty and effort necessary during reading tasks (Shaywitz et al. 1998; Brunswick et al. 1999; Milne et al. 2002). This compensatory theory is supported by findings of more prominent hyperactivation in older, or remediated, readers (Shaywitz et al. 2003; Hoeft et al. 2011; Richlan et al. 2011; Barquero et al. 2014).

The goal of the present study was to comprehensively investigate whether variability in TPJ functional connectivity is an indicator of reading competence in a community sample of adults for whom brain network development and reading skill has reached a relatively stable plateau. To this end, we used resting-state fMRI and a connectivity-based clustering approach to identify subregions around the TPJ with distinct, and relatively homogeneous, connectivity patterns. These regions were used to study the relationship between TPJ connectivity and reading measures in a community sample of adults spanning a wide range of reading abilities. We were particularly interested in testing whether TPJ functional connectivity differences would implicate regions also identified as structurally or functionally abnormal in meta-analyses of RD (Richlan et al. 2009, 2011).

Task-independent connectivity analyses can provide insight into circuit dysfunction, independent of performance. Associations between reading skill and TPJ connectivity with insular, prefrontal, or subcortical regions could help account for findings from task-based meta-analyses of RD. For example, if hyperactive frontal, striatal, and insular regions are epi-phenomenal and not specifically related to phonological compensation, we might not expect to find connectivity differences with left TPJ networks in weaker readers at rest. If, on the other hand, this hyperactivation is compensatory, that is cortico–subcortical networks are consistently overengaged due to increased effort required during reading, we might expect enhanced left TPJ to prefrontal, insular, and subcortical connectivity in weaker readers. By investigating a community sample of adults, our results can provide insight into the long-term outcomes in individuals who have likely experienced reading difficulties since childhood.

To address this question, we used connectivity-based clustering (Mars et al. 2011; Bray et al. 2013) to identify subdivisions within the TPJ with relatively homogeneous connectivity profiles. As previous studies have reported 3 functional subdivisions within the TPJ (Mars et al. 2012), with connectivity to the default-mode, salience, and ventral attention networks, we first report results using a 3-cluster solution as seeds. We additionally tested a higher resolution parcellation (8 subregions), which we hypothesized might reveal TPJ subnetworks with more specific connectivity patterns to regions involved in reading.

Methods

Participants and Cognitive Assessments

Participants were 48 adult humans ranging from 30 to 54 years of age, all of whom provided written consent to participate in this study using a form approved by the Institutional Review Board at the University of California, San Francisco and Stanford University. Participants were recruited through advertisements in the San Francisco Bay Area for individuals with a family history of reading difficulties and their unaffected spouses. Three participants were excluded due to motion artifacts, and cognitive measures were not collected for 1 participant, leaving a final sample of 44 (22 males). This final sample had a mean age of 43.0 ± 6.9 and included 5 left-handed and 2 ambidextrous participants, based on self-report. All participants were administered the Wechsler Abbreviated Scale of intelligence (WASI) (Wechsler 1999). Full-scale IQ (FIQ) was normal to above average for all participants with a mean of 121 ± 8.2 and a range from 105 to 134. Additional assessments of reading and spelling were acquired: the Test of Word Reading Efficiency (TOWRE) 2nd edition (Torgesen et al. 1999), Phonemic Decoding and Sight Word Efficiency subtests (PDE and SWE), the Adult Reading History Questionnaire (ARHQ) (Lefly and Pennington 2000), the Woodcock-Johnson IIIA Spelling subtest (WJ-SP) (McGrew and Woodcock 2001), Rapid Automatized Naming (RAN) of Numbers (RAN-N) and Letters (RAN-L) (Wolf and Denckla 2005), the Woodcock Reading Mastery Test (WRMT) (Woodcock 1987, 25), and the Peabody Picture Vocabulary Test (PPVT) (Dunn and Dunn 1997). Detailed participant characteristics are provided in Table 1, where we note the

Table 1 Detailed participant characteristics

Measure	All participants ($n = 44$)			
	Mean (SD)	Score range	No. of participants below cutoff	No. of participants above cutoff
Age	43.5 (5.5)	30 to 54		
FIQ	121.1 (8.2)	105 to 134		
TOWRE-PDE (SO)	93.09 (9.54)	71 to 112	15	1
TOWRE-SWE (SO)	96.1 (12.11)	71 to >113	12	14
WJIIIA spelling (S)	107.5 (9.0)	83 to 128	1	15
Rapid naming numbers (SO)	112.3 (5.16)	102 to 126	0	27
Rapid naming letters (SO)	108.43 (3.4)	97 to 120	0	16
WRMT-Word identification (S)	104.1 (7.8)	85 to 121	2	6
WRMT-Passage comprehension (S)	111.5 (8.7)	91 to 135	0	27
WRMT-Word attack (S)	106.3 (6.8)	93 to 118	0	12
PPVT (S)	111.4 (9.0)	93 to 132	0	26
ARHQ (cutoff at 0.4)	0.34 (0.13)	0.09 to 0.66		14

Note: Mean and standard deviation (SD) for age, FIQ, and scores on reading and vocabulary measures are detailed. (S) indicates that standard scores are provided; since the TOWRE and Rapid Naming tests do not have published norms for adults, scores were standardized using the oldest available age as a reference, indicated as (SO). The 2 rightmost columns indicate the number of participants <90 or >110 on standardized scores. For the ARHQ, the number of participants ≥0.4 is noted (Maurer et al. 2003; Black et al. 2012). TOWRE, Test of Word Reading Efficiency; PDE, phonemic decoding efficiency; SWE, sight word efficiency; WJIIIA, Woodcock-Johnson IIIA; WRMT, Woodcock reading mastery test; PPVT, Peabody picture vocabulary test; ARHQ, adult reading history questionnaire.

number of participants who scored below 90 (bottom 25th percentile) or above 110 (upper 25th percentile) on standardized reading measures. Four participants reported a previous diagnosis of dyslexia, 1 a diagnosis of learning disorder other than dyslexia, and 2 a diagnosis of attention deficit hyperactivity disorder (ADHD).

Rather than splitting our data into groups of stronger and weaker readers based on reading scores, we based our analyses on regression models to assess the relationship between functional connectivity and continuous reading measures. We refer to weaker readers as those scoring at the lower end of this continuum, and stronger readers as those scoring at the upper end. Since measures such as timed pseudoword decoding are sensitive indicators of phonological processing, TOWRE-PDE was used as the main regressor of interest for functional connectivity analyses, and standard scores were obtained using the oldest available age norm as reference. Regression analyses demonstrated no significant relationships between age and raw scores, and factor analysis of reading-related measures, described in the next paragraph, loaded onto a common factor, justifying the appropriateness of using this measure.

To assess generality of our findings to reading skill, a composite reading skill score was generated. This score was derived using a principal components analysis on the following standard scores: TOWRE-PDE, WJ-SP, WRMT-Word identification, WRMT-Word attack, and WRMT-Passage comprehension. The first principal component accounted for 61% of the variance in the data and had loadings of [0.82, 0.84, 0.89, 0.64, 0.65] on the respective scores.

MRI Data Acquisition

MRI data were collected at Stanford University using a GE Healthcare 3.0 Tesla 750 scanner and an 8-channel phased array head coil (GE Healthcare, Waukesha, WI, USA). Anatomical images were acquired using an axial-oblique 3D T_1-weighted sequence (fast spoiled gradient recalled echo [FSPGR] pulse sequence, inversion recovery preparation pulse [TI] = 400 ms; repetition time [TR] = 8.5 ms; echo-time [TE] = 3.4 ms; flip angle = 15°; slice thickness = 1.2 mm; 0.86 × 0.86 mm in-plane resolution; 128 slices; number of excitations = 1; field-of-view [FOV] = 22 cm; acquisition matrix = 256 × 192; duration = 4:54 min). Resting-state functional MRI (fMRI) data were acquired, with the subjects' eyes closed, using an axial 2D GRE Spiral In/Out (SPRLIO; Glover and Law [2001]) pulse sequence (TR = 2000ms; TE = 30 ms; flip angle = 80°; slice thickness = 4.0 mm; number of slices = 31, descending; 3.44 × 3.44 mm in-plane resolution; number of temporal frames = 180; FOV = 22 cm). The duration of the resting scan was 6 min.

fMRI Preprocessing

Functional images were preprocessed using SPM8 software (http://www.fil.ion.ucl.ac.uk/spm/software/spm8/) in MATLAB (Mathworks, Natick, MA, USA). Images were corrected for slice timing and realigned to the first scan in the functional series. Preprocessed images were analyzed with Art software to identify volumes with >0.2 mm/TR scan-to-scan motion, which were excluded from correlation, and de-weighted in regression, models, and to calculate the mean frame-wise displacement (FD) for each participant. The number of excluded volumes ranged from 0 to 70. Supplementary Figure 1 shows the mean FD and number of excluded volumes across the sample. As described below, reading measures were regressed against functional connectivity patterns. Importantly, the number of frames excluded did not significantly correlate with reading measures (TOWRE-PDE: $r = -0.04$, $P = 0.8$; RAN-N: $r = 0.0491$ and $P = 0.7517$). Each participant's T_1 anatomical scan was co-registered to the mean functional image of each run and segmented to obtain the CSF, gray, and white matter images, as well as normalization parameters to the Montreal Neurological Institute (MNI) template. For connectivity analyses, nuisance regression was applied to obtain residualized images. Nuisance regressors included motion parameters estimated during realignment (standard 6 parameter model), and time courses from cerebrospinal fluid (CSF) and white matter, extracted by averaging the signal at each time point over the voxels of a particular tissue type (CSF or white matter) from the individual's segmented images. A linear trend was subtracted to account for linear drift over time, and a low pass filter of 0.1 Hz applied. Spatial normalization parameters from the segmentation

process were used to normalize the realigned functional images to Montreal Neurological Institute (MNI) template space. Normalized images were smoothed with a 6 mm FWHM Gaussian kernel.

TPJ Mask Creation

A mask encompassing the left TPJ region was created consisting of the inferior parietal lobule (IPL), supramarginal gyrus (SMG), and angular gyrus (AG) as defined in the Automated Anatomical Labeling (AAL) atlas (Maldjian et al. 2003) using the Wake Forest University (WFU) PickAtlas tool (http://fmri.wfubmc.edu/software/PickAtlas). The TPJ mask also included a posterior region of the superior temporal gyrus (STG) and an anterior portion of the middle occipital gyrus (MOG). These were added by including the respective anatomical masks for these regions but truncating the STG to only include the most posterior portion (posterior to MNI coordinate $y = -18$), and the MOG to only include the most anterior portion (anterior to MNI coordinate $y = -84$). Finally, a small gap between the posterior STG and MOG was manually filled in. A right TPJ mask was created as the mirror image of the left.

Cluster-Based Definition of TPJ ROIs

The TPJ was divided into clusters of voxels showing similar whole-brain connectivity profiles using k-means clustering in MATLAB. To reduce computation time, images were resampled to 4 mm^3 voxels prior to clustering (connectivity models described in subsequent sections used 2 mm^3 voxel images). A correlation matrix was generated for each participant in which each row corresponded to a voxel in the TPJ mask, each column corresponded to a voxel in the rest of the brain, and each matrix entry contained the correlation between time courses for the 2 corresponding voxels. These correlation matrices were averaged across the group and entered into k-means clustering. Clusters were generated from connectivity averaged across the entire sample, rather than in stronger and weaker readers separately, so that seed regions for connectivity analyses would be consistent across the sample, and avoid introducing bias in the location/extent of seed regions between groups. K-means clustering starts with a particular assignment of rows to clusters and iterates, re-assigning each row to the cluster whose center it is nearest to, until no further reassignment takes place. Here, the k-means algorithm started with random assignment and was run 10 times, to find the assignment that minimized the total distance to center. As previous structural connectivity literature has suggested that 3 large-scale networks make connections with the TPJ (Mars et al. 2012), the left and right TPJ were initially divided into 3 networks. As these clusters were relatively large, a more fine-grained parcellation was subsequently conducted. An 8-cluster solution was chosen as this was the minimum >3 that contained contiguous clusters in both hemispheres.

TPJ Clustering: 3-Cluster Solution

Clustering of left and right TPJ resulted in 3 relatively symmetric clusters. The center of mass, size, and corresponding AAL label (Tzourio-Mazoyer et al. 2002) for each cluster are shown in Table 2. We observed an anterior cluster covering the SMG/IPL (orange in the central panels of Fig. 1), a posterior cluster covering the AG (green) and an inferior cluster covering the posterior superior temporal sulcus (STS) (violet). Average time courses from each of these clusters were regressed against whole brain signals to identify associated connectivity patterns, shown in the periphery of Figure 1. The network corresponding to the orange/SMG cluster included bilateral intraparietal sulcus, anterior insula, and dorsal prefrontal regions, consistent with the dorsal attention or fronto-parietal network (DAN; Power et al. [2011]). This network also included a bilateral occipito-temporal region that has been associated with orthographic processing (McCandliss et al. 2003), but recent work suggests that it is also integrated with the DAN at rest (Vogel et al. 2012). This network was anticorrelated with posterior cingulate, medial prefrontal, and anterior caudate regions (shown in blue). The AG/green network was associated with medial prefrontal and posterior cingulate/precuneus regions similar to the default-mode network or task negative system (DMN; Fox et al. [2005]; Power et al. [2011]). This network was anticorrelated with visual, insular, and cingulate regions. The third, pSTS/violet cluster was associated with regions of the salience network (Seeley et al. 2007; Sridharan et al. 2008) including cingulate cortex and insula, but also showed positive connectivity to visual, motor, and superior parietal regions as well as thalamus (visible on lower right panel).

TPJ Clustering: 8-Cluster Solution

The left and right TPJ were separately divided into 8 subregions. The networks associated with each cluster are shown in Figure 2 (left) and Supplementary Figure 2 (right); the center of mass, size, and AAL label for each cluster are shown in Table 3. Similar to the 3-cluster solution, we identified subregions in both hemispheres with connectivity to regions of the DMN (green), DAN (orange), and cingulo-opercular or salience network (violet). Additional subregions were identified with connectivity to visual (light purple) and STS regions (blue). Finally, several subregions had connectivity patterns not typically seen in canonical networks, such as post-central + cingulate + parietal (red), insula + cingulate + visual + motor + thalamus (cyan) and posterior cingulate + inferior parietal + dorsal prefrontal (yellow). Similar to the 3-cluster case, several subregions also showed significant anticorrelation

Table 2 Cluster information: 3-cluster solution

Cluster	Center of mass (X,Y,Z), mm	Size, mm^3	Color in Figure 1	AAL label
Left				
1	−51, −44, 20	37 488	Violet	Superior temporal
2	−45, −45, 42	24 496	Orange	Inferior parietal lobule
3	−44, −63, 34	25 672	Green	Angular gyrus
Right				
1	49, −45, 21	36 488	Violet	Superior temporal
2	44, −47, 41	25 568	Orange	Inferior parietal lobule
3	47, −9, 33	27 208	Green	Angular gyrus

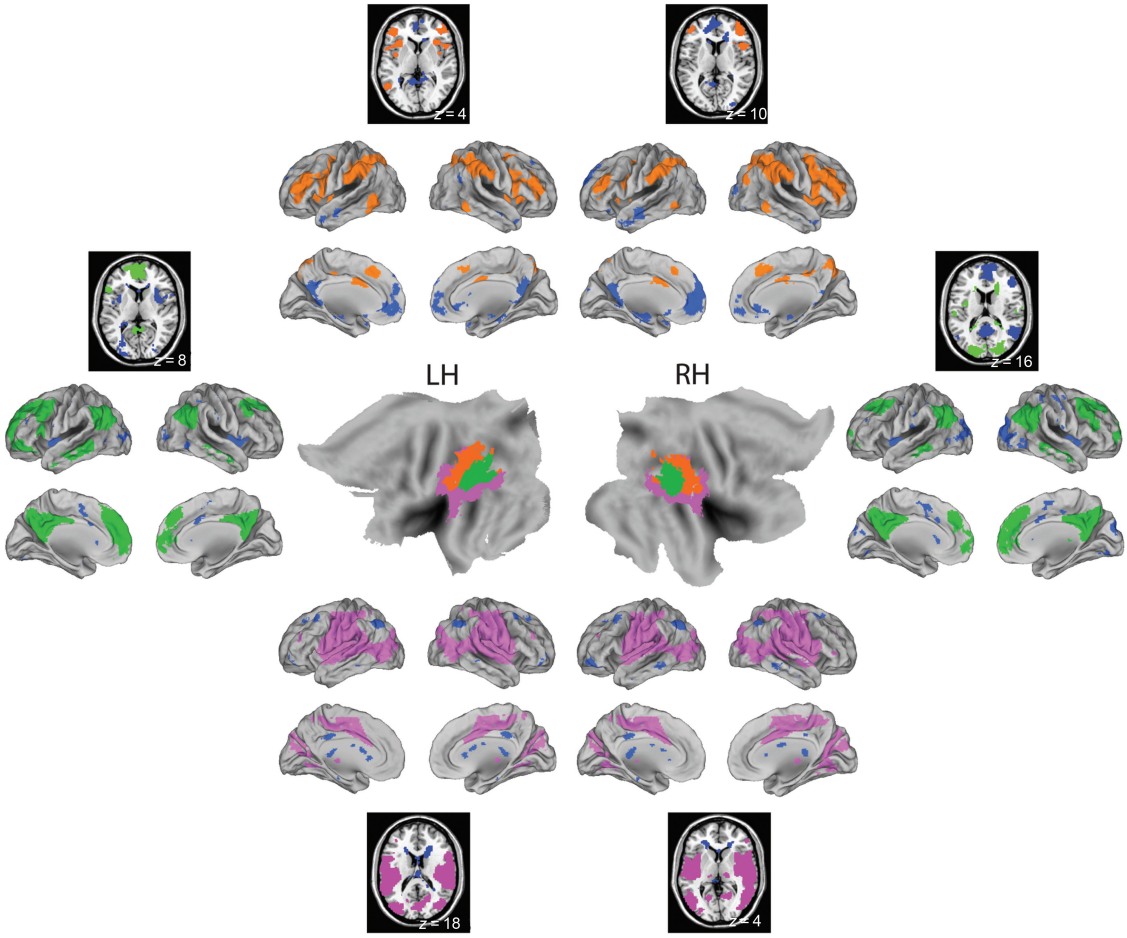

Figure 1. TPJ clusters and associated networks for 3-cluster solution. Central panels show TPJ clusters for the left and right hemispheres overlaid on inflated and flattened brains (posterior pointed toward the center). Detailed information about seed clusters is presented in Table 2. Each cluster was used as a seed to identify an associated network across the group. These are shown around the periphery, on cortical surfaces, color-coded to match central clusters. Significant negative associations are shown in dark blue across all panels. The green (angular gyrus) cluster was associated with posterior cingulate, medial prefrontal, and inferior parietal DMN regions. The violet (superior temporal) cluster showed connectivity with cingulate and insular regions of the salience network. The orange (anterior/IPL) cluster was associated with intraparietal sulcus and dorsal prefrontal regions typically linked with the DAN or fronto-parietal network. These are similar to networks identified in Mars et al. (2012). Network overlays are thresholded at $P < 0.05$ FWE-corrected. LH, left hemisphere; RH, right hemisphere; DMN, default-mode network; DAN, dorsal attention network; IPL, inferior parietal lobule; TPJ, temporo-parietal junction.

patterns (shown in dark blue on all peripheral panels), including subcortical and insular regions.

Functional Connectivity Models Using Cluster-Derived TPJ Regions-of-Interest

Regions of interest (ROIs) were defined from each cluster obtained from group-level parcellation of the TPJ. As described above, we used 2 clustering analyses: a 3-cluster solution to replicate a prior study of connectivity-based TPJ parcellation (Mars et al. 2012), and a more fine-grained 8-cluster solution. Association with decoding measures was examined for both solutions. Time courses were extracted by averaging over all voxels in an ROI at each time point; time-course extraction and subsequent models were performed in MNI space. These time courses were entered as regressors in a general linear model for each ROI and subject. Group-level between-subjects multiple regression models were conducted to assess relationships between connectivity of each TPJ cluster to TOWRE-PDE scores. These models included handedness (2 columns with ones for left-handed or ambidextrous participants), sex (1 = male), age, FIQ, and mean frame-wise displacement as covariates of no interest. Inferences were drawn at a height threshold of $P < 0.001$ uncorrected and cluster-level multiple comparisons correction set at $P < 0.05$ Family Wise Error (FWE) corrected. Results were overlaid on inflated cortical surfaces using caret software. This composite score was used in a second set of multiple regression models to assess generalizability of PDE findings to overall reading skills. Finally, as PDE scores may also depend on processing speed, a third set of models assessed specificity by using RAN-N, a measure of speeded naming and processing speed, as a regressor.

As previous work has shown reduced functional connectivity between left inferior frontal gyurs (IFG) and parietal language regions in individuals with RD or weaker reading skill (Koyama et al. 2011; Boets et al. 2013; Schurz et al. 2014), we examined positive associations between PDE scores and connectivity from all left hemisphere seed regions to the left IFG at a reduced threshold of $P < 0.001$ uncorrected.

Results

3-Cluster Seed Correlations with Pseudoword Decoding

Regression models with pseudoword decoding scores identified, in the left hemisphere, a significant negative correlation with PDE

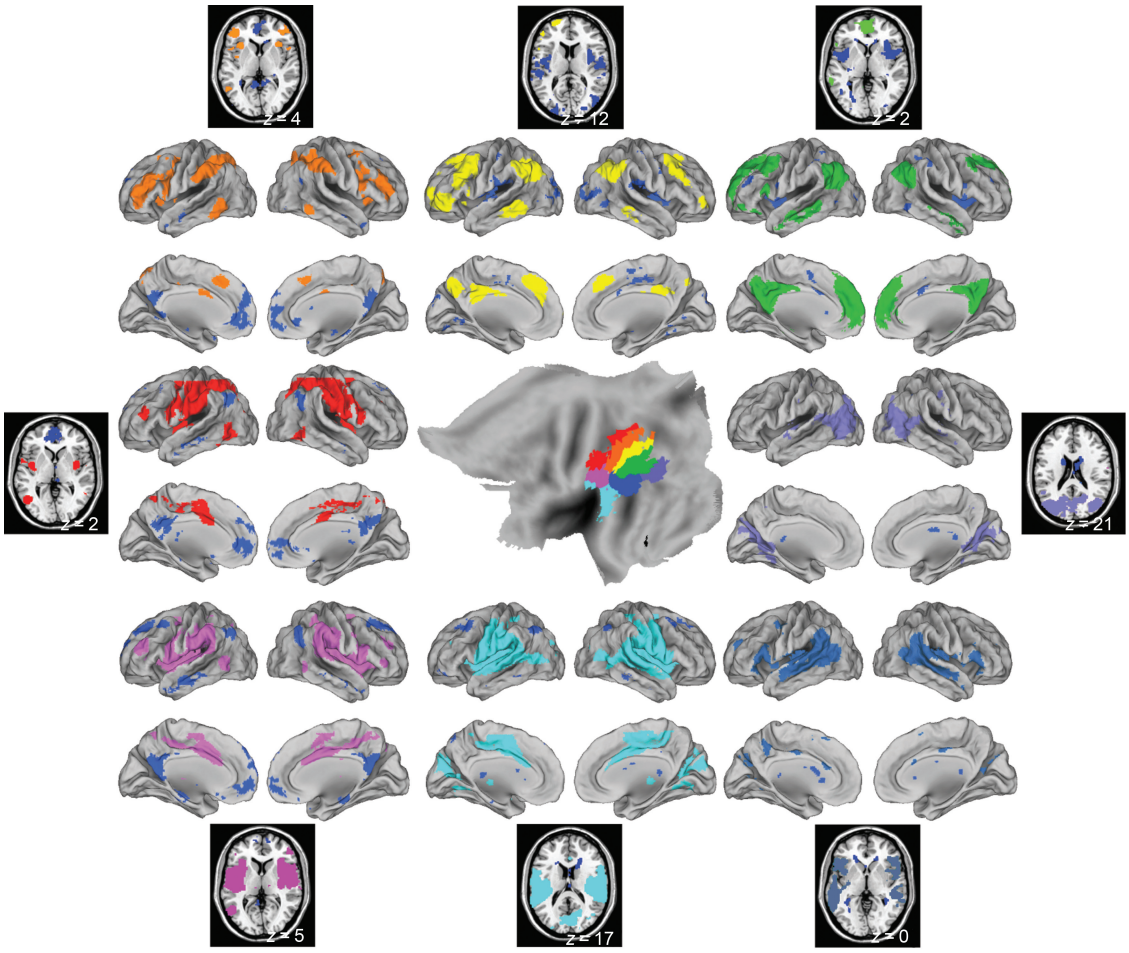

Figure 2. TPJ clusters and associated networks for 8-cluster solution, left hemisphere. Central panels show TPJ clusters for the left hemisphere overlaid on an inflated hemisphere (posterior pointed toward the right). Detailed information about seed clusters is presented in Table 3. Each cluster was used as a seed to identify the associated network across the group. These are shown around the periphery, on cortical surfaces, color-coded to match central clusters. Significant negative associations are shown in dark blue across all panels. These networks resemble the DMN (green), DAN (orange), salience (violet), similar to the 3-cluster solution. Visual (light purple) and STS (blue) networks emerged, as well as networks with connectivity patterns that do not correspond to canonical networks (red, yellow, cyan). Network overlays are thresholded at $P < 0.05$ FWE-corrected. DMN, default-mode network; DAN, dorsal attention network; STS, superior temporal sulcus; TPJ, temporo-parietal junction.

Table 3 Cluster information: 8-cluster solution

Cluster	Center of mass (X,Y,Z), mm	Size, mm^3	Color in Figure 2	AAL label
Left				
1	−45, −34, 44	12 168	Red	Inferior parietal lobule
2	−43, −47, 45	13 424	Orange	Supramarginal gyrus/inferior parietal lobule
3	−42, −58, 44	11 576	Yellow	Angular gyrus
4	−44, −65, 30	16 200	Green	Posterior angular gyrus
5	−52, −52, 17	10 760	Blue	Middle temporal
6	−56, −31, 14	11 560	Cyan	Superior temporal
7	−41, −73, 15	9536	Light purple	Middle occipital
8	−58, −34, 29	9728	Violet	Supramarginal
Right				
1	40, −46, 42	16 704	Red	Inferior parietal lobule
2	46, −46, 44	13 416	Orange	Supramarginal gyrus/inferior parietal lobule
3	50, −58, 29	12 104	Yellow	Superior angular gyrus
4	42, −63, 41	13 496	Green	Angular gyrus
5	51, −54, 17	13 368	Blue	Middle temporal
6	56, −30, 14	11 008	Cyan	Superior temporal
7	40, −73, 15	8848	Light purple	Middle occipital
8	59, −31, 31	8408	Violet	Supramarginal

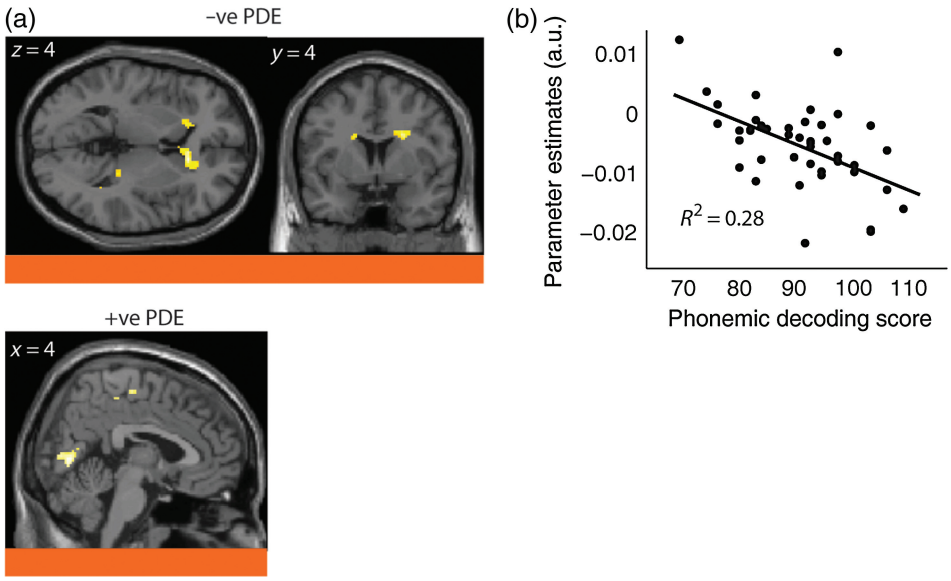

Figure 3. Correlations between 3-cluster seeds and phonemic decoding scores. (*a*) Negative correlation between left SMG/IPL seed and bilateral caudate head ([12, 26, 6], $n = 245$, $Z = 4.78$), and right dorsal caudate ([22, 4, 28], $n = 142$, $Z = 4.26$); positive association for this cluster with PDE scores in pericalcarine cortex ([4, −72, 4], $n = 152$, $Z = 3.76$) in lower panel. Panels are color-coded to match seed regions from Figure 1. (*b*) Scatter plot of parameter estimates from the peak anterior caudate voxel against phonemic decoding scores, with least squares regression line. IPL, inferior parietal lobule; SMG, supramarginal gyrus; PDE, phonemic decoding efficiency.

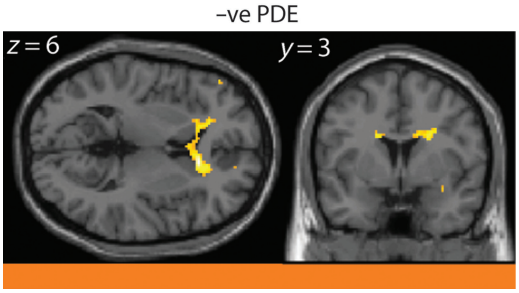

Figure 4. Correlations between left hemisphere 8-cluster seeds and phonemic decoding scores. Significant negative association between IPL to bilateral caudate head ([12, 26, 6], $Z = 5.19$ and [−18, 28, 0], $Z = 4.4$, $n = 506$) and right dorsal caudate ([22, 4, 28], $n = 215$, $Z = 4.42$) connectivity and phonemic decoding scores. Panel is color-coded to match TPJ cluster seed regions from Figure 2. TPJ, temporo-parietal junction; PDE, phonemic decoding efficiency; IPL, inferior parietal lobule.

scores using the left anterior SMG/IPL cluster (orange in Fig. 1) with bilateral caudate head ([12, 26, 6], $n = 245$, $Z = 4.78$; Fig. 3) and right dorsal caudate ([22, 4, 28], $n = 142$, $Z = 4.26$). This cluster survived small volume correction in a 10-mm sphere around the right caudate peak reported as hyperactive in RD in a recent meta-analysis (Tailarach: [16, 10, 10]; Richlan et al. [2011]). We also found a positive association for this cluster with PDE scores in pericalcarine cortex ([4–72, 4], $n = 152$, $Z = 3.76$). Both significant effects were located in regions on average anticorrelated with the SMG cluster across the group, as seen in blue in the top panels of Figure 1. No significant effects were found for right hemisphere clusters.

An ROI analysis in the left IFG pars opercularis identified a cluster from only the SMG/IPL (orange) seed at $P < 0.001$ uncorrected ([−54, 24, 8], $n = 15$, $Z = 3.74$), consistent with the previous literature.

8-Cluster Seed Correlations with Pseudoword Decoding

Multiple regression models investigated correlations between PDE scores and connectivity patterns with each of 16 seed regions (8 in each hemisphere). In the left hemisphere (Fig. 4), from the SMG/IPL cluster (orange in Fig. 2), negative correlations with PDE scores were observed in bilateral caudate head ([12, 26, 6], $Z = 5.19$ and [−18, 28, 0], $Z = 4.4$, $n = 506$), similar to the results from the 3-cluster solution. Additional negative effects for this cluster were found in right dorsal caudate ([22, 4, 28], $n = 215$, $Z = 4.42$), and in several white matter regions adjacent to anterior and posterior caudate ([−30–8 32], $n = 118$, $Z = 4.95$; [−30, −36, 22], $n = 208$, $Z = 4.89$; [−22, 20, 18], $n = 193$, $Z = 4.23$). Significant negative effects in the caudate were located in regions that are on average anticorrelated with the TPJ seeds (top left panels in Fig. 2). That is, in weaker readers, these regions were less anticorrelated. Also similar to the 3-cluster solution, the SMG/IPL (orange) cluster showed a positive correlation with PDE scores in left IFG pars opercularis at a reduced threshold of $P < 0.001$ uncorrected ([−54, 24, 8], $n = 18$, $Z = 3.7$). In the right hemisphere, a positive correlation with PDE scores was observed in connectivity between the AG cluster and left occipito-temporal cortex ([40, −68, 10], $n = 14$, $Z = 4.0$; Fig. 5). This effect was located in a region on average anticorrelated with the seed.

3-and 8-Cluster Seed Correlations with Composite Reading Skill Score

To assess generality of these findings to reading skill, similar models were run using a composite reading score. Significant effects for these models are shown in Supplementary Figures 3–5. This analysis replicated the caudate findings reported for PDE scores and identified additional significant correlations. For the 3-cluster solution, only the left IPL/SMG cluster showed significant negative associations with reading scores, in bilateral caudate head ([16, 34, 6], $n = 1093$, $Z = 5.2$), and dorsal caudate ([24, 10, 20], $n = 209$, $Z = 4.2$). For the 8-cluster solution, again, in the left hemisphere, from the SMG/IPL cluster (orange in Fig. 2), negative correlations were observed in bilateral caudate head ([16, 34, 6], $Z = 5.7$ and [−18, 28, 0], $Z = 5.0$, $n = 1686$). A second cluster (AG; yellow in Fig. 2) showed a similar negative relationship to bilateral caudate head ([12, 30, 0], $n = 377$, $Z = 4.4$; [−18, 26, 2], $n = 368$,

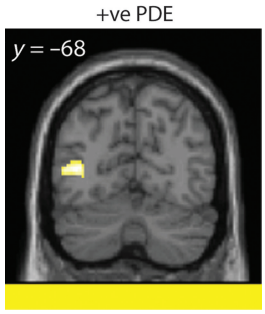

Figure 5. Correlations between right hemisphere 8-cluster seeds and phonemic decoding scores. Significant positive association between AG to left occipito-temporal ([12, 28, 6], $n = 133$, $Z = 4.5$) connectivity and phonemic decoding scores. Panel is color-coded to match TPJ cluster seed regions from Figure 2. AG, angular gyrus; PDE, phonemic decoding efficiency; TPJ, temporo-parietal junction.

$Z = 4.1$), in addition to a significant positive correlation with PDE scores in right temporal cortex ([50, −66, 20], $n = 115$, $Z = 4.6$). In the right hemisphere, we found a negative correlation between the IPL/SMG cluster (orange) and right anterior caudate ([12, 28, 6], $n = 133$, $Z = 4.5$). Positive correlations were found between the IPL (red) cluster and left middle frontal gyrus ([−34, 42, 14], $n = 147$, $Z = 4.6$) between the superior AG cluster (yellow) and left occipito-temporal cortex and calcarine sulcus ([−38 −68, 8], $n = 150$, $Z = 4.3$; [2, −88, 10], $n = 195$, $Z = 4.3$) and between the middle occipital (light purple) cluster and left TPJ ([−50, −46, 40], $n = 112$, $Z = 4.3$).

3-and 8-Cluster Seed Correlations with RAN-N Scores

To assess specificity of these findings compared with another reading-related measure but independent from decoding measures, similar models were run using all 6 and 16 bilateral clusters that form the 3- and 8-cluster solutions, and speeded naming and processing speed (RAN-N scores) as the regressor of interest. For the 3-cluster solution bilaterally, no significant effects were observed. For the 8-cluster solutions, results showed that only one right hemisphere cluster had a significant negative correlation with this measure in left occipito-temporal cortex ([−48 −62 −12], $n = 134$, $Z = 4.3$). In a set of models including both PDE and RAN-N scores, the anterior caudate clusters reported above remained significantly associated with PDE scores and showed no significant association with RAN-N scores (at $P > 0.001$ uncorrected). Thus, the significant relationship between SMG/IPL to anterior caudate connectivity observed for TOWRE-PDE and composite reading skill scores was not apparent for RAN-N scores.

Discussion

The left TPJ is a core region implicated in reading and RD (Maisog et al. 2008; Richlan et al. 2009, 2011), yet variation in TPJ network connectivity has not been comprehensively investigated in relation to reading abilities. Using a data-driven connectivity clustering approach to define subregions around the TPJ, we found that connectivity between bilateral IPL/SMG and caudate head showed a negative association with phonemic decoding and reading skill scores (i.e., worse reading skill is reflected in less negative connectivity). Additional findings were that inter-hemispheric TPJ connectivity and right TPJ to left prefrontal and peri-calcarine cortex connectivity were positively correlated with PDE scores (i.e., worse performance was reflected in less positive connectivity). The identified relationships between functional connectivity of subnetworks around the TPJ and reading skill adds to our understanding of interindividual variability in reading competence and help to reconcile findings from functional imaging meta-analyses of RD of co-occurring underactivation near the TPJ and overactivation in subcortical regions.

We note that while 4 participants reported a historical diagnosis of dyslexia and 14 scored above 0.4 on the ARHQ (Maurer et al. 2003; Black et al. 2012), the present study did not directly contrast participants with RD against typical readers. Thus, it is perhaps not clear whether our findings would extend to a group comparison of typical readers against adults with a clear diagnosis of RD. That said, several authors have pointed out that reading measures in adults tend to be continuous rather than dichotomous (Rodgers 1983; Jorm et al. 1986; Stevenson 1988; Shaywitz et al. 1992; Fletcher 2009), suggesting that a correlation approach is appropriate for investigations of reading, and can provide insight into the neural bases of RD.

The dorsal caudate has been highlighted as consistently overactive in RD (Kronbichler et al. 2006; Hoeft et al. 2007; Richlan et al. 2009, 2011); we note that the PDE-associated connectivity identified here survived small volume correction around the right caudate peak reported as hyperactive in RD in a recent meta-analysis (Richlan et al. 2011). Functionally the caudate, or dorsal striatum, has been implicated in implicit learning (Nicolson et al. 2010) and in word, relative to spatial, interference (Ali et al. 2010). In our analyses, the SMG/IPL seed was associated with regions of the dorsal attention or fronto-parietal network and was anticorrelated with anterior caudate at rest, but less so in weaker readers, possibly indicating an overintegration of anterior caudate into fronto-parietal attention networks. Increased functional connectivity between left IFG and left caudate in RD has also been reported (Finn et al. 2013). Given the connectivity profile of the TPJ subregion showing this effect, and the fact that caudate hyperactivation appears more prominently in meta-analyses of adult relative to child RD studies (Richlan et al. 2011), our results support a hypothesis that a long-term increase in effortful articulatory processing (Shaywitz et al. 1998; Brunswick et al. 1999; Milne et al. 2002) has resulted in reduced anticorrelation, or inhibition, between fronto-parietal attention networks and caudate head in weaker readers. An alternative interpretation is that this anticorrelated subcortical/cortical network simply shows a reduced organization in less skilled readers. A longitudinal study would be required to tease apart the long-term effects of compensation strategies on connectivity patterns.

Several task-based neuroimaging studies of RD have interpreted overengagement of regions such as the caudate and inferior frontal gyrus as compensatory (Shaywitz et al. 1998, 2002; Brunswick et al. 1999; Hoeft et al. 2007). In addition to caudate findings, we also replicated findings of reduced TPJ to IFG functional connectivity in RD (Boets et al. 2013). This disconnection at rest may imply differences in properties of connecting white matter (Boets et al. 2013) that require compensatory overengagement of TPJ and IFG to achieve the same level of information transmission. Thus, together with the caudate findings, we observed both weaker positive and negative correlation between the TPJ and regions previously reported to show hyperactivation in task-based studies.

It has been suggested that the phonological deficit may be best understood as a difficulty with phonemic retrieval rather than representation (Boets et al. 2013; Boets 2014), with retrieval difficulties caused by underconnectivity of left hemisphere language and auditory regions. In the present study, we also found a correlation between left TPJ to IFG connectivity and PDE scores,

at a statistical threshold appropriate for an a priori ROI. Findings regarding the relationship between task-independent functional connectivity of left temporo-parietal cortex and left IFG and reading skill have been mixed (Koyama et al. 2011, 2013; Boets et al. 2013; Finn et al. 2013; Schurz et al. 2014). Connectivity between BA39 and Broca's region has been shown to correlate more strongly with reading measures during reading tasks relative to rest (Hampson et al. 2006), though consistent connectivity differences in RD across both task and resting conditions has also been shown (Schurz et al. 2014). It is also notable that several studies have used residualized task-based scans rather than resting scans (Boets et al. 2013; Finn et al. 2013), potentially contributing to inconsistent findings across "task-independent" connectivity studies.

Alternative theories have suggested that RD is rooted in abnormalities in visual processing (Demb et al. 1998) and visual-spatial attention (Facoetti et al. 2000; Franceschini et al. 2012). In the present study, right hemisphere connectivity between AG and pericalcarine cortex positively correlated with phonemic decoding. Aberrant connectivity of visual regions in RD has also been shown in several recent reports (van der Mark et al. 2011; Finn et al. 2013; Fan et al. 2014; Schurz et al. 2014). Deficits in basic visual processing have long been linked with RD, particularly in the magnocellular pathway (Demb et al. 1998). Recently a genetic risk factor for developmental dyslexia, a deletion in intron 2 of the DCD2 gene, has been linked to impaired illusory motion processing, a magnocellular dorsal stream function (Gori et al. 2015). The most prominent findings here were aberrant connectivity between anterior caudate and a TPJ subregion functionally connected to DAN regions such as the intraparietal sulcus, putative human frontal eye fields, and dorsolateral prefrontal cortex. Many studies have highlighted abnormalities in visuospatial attention in RD (Facoetti and Molteni 2001; Hari et al. 2001; Facoetti et al. 2003, 2006; Sireteanu et al. 2005; Liddle et al. 2009; Facoetti, Corradi et al. 2010; Facoetti, Trussardi et al. 2010). Converging evidence also suggests that difficulties in visuospatial attention are an important predictor of reading abilities (Valdois et al. 2004; Shaywitz and Shaywitz 2008; Franceschini et al. 2012, 2013). Reading remediation (Franceschini et al. 2013) may rely largely on alterations in visual or auditory attentional functions of the dorsal attention network (Ronconi et al. 2014). Our findings indicate that integration between fronto-parietal attention networks and visual and subcortical regions is an important predictor of phonological processing and reading skills.

A set of left-lateralized cortical regions has consistently been implicated in language and reading (Ojemann et al. 1989), and structural abnormalities in left hemisphere regions in pre-reading children may predict later reading difficulties (Clark et al. 2014). However, some studies that have applied network analyses to resting functional connectivity have not found evidence for a dedicated reading network (Vogel et al. 2012, 2013). Regions involved in reading are members of default-mode, visual, motor, and fronto-parietal networks (Vogel et al. 2013). A theoretical framework has been proposed for language more generally (Fedorenko and Thompson-Schill 2014), in which a core set of "language" regions may functionally interact with a set of domain general regions during the performance of language tasks. In support of this view, the correlates of phonemic decoding identified here were not specifically localized to language regions, but rather were distributed across visual, fronto-parietal attention, and default-mode network associated regions of the TPJ.

The TPJ region of interest was initially divided into 3 subregions with connectivity patterns similar to those described in previous work (Mars et al. 2012; Bzdok et al. 2013): an anterior cluster connected to fronto-parietal attention network regions such as dorsolateral prefrontal cortex and intraparietal sulcus, a posterior cluster connected with DMN-associated regions such as medial prefrontal/anterior cingulate cortex and posterior cingulate cortex and an inferior cluster with cingulo-opercular regions resembling the "salience" network (Seeley et al. 2007). When moving to the 8-cluster solution, 2 more focused visual and STS networks were identified (light purple, blue), while the DMN (green) and DAN (orange) remained. The salience (violet) network became more focused and networks with intermediate connectivity were apparent (red, yellow, cyan). The TPJ divisions observed here are consistent with a recent parcellation of left lateral parietal cortex (Nelson et al. 2010). The TPJ is located at the intersection of several large-scale networks in the brain, and it has been suggested that these regions of high community density have a privileged "hub" position by linking several brain networks (Power et al. 2013; Bray et al. 2015). It is notable that an intermediate DAN/DMN (yellow) cluster was among those that showed a positive correlation with phonemic decoding scores in visual regions. This region may play an important role in linking multiple functional networks, with implications for complex skills such as phonemic decoding.

The left and right TPJ are often considered separately in neuroimaging studies, partly due to differences in their attributed functions. Regions near the left TPJ are known to play a role in aspects of language (Binder et al. 1997), semantics (Binder et al. 2009), and reading (reviewed in Price [2012]). Left SMG has been implicated in phonological processing (McDermott et al. 2003), articulatory rehearsal (Démonet et al. 1994), and linking basic components of vocabulary knowledge (Lee et al. 2007), the AG in semantic processing (Vandenberghe et al. 1996), and the posterior STG in early auditory processing and speech perception (Fiez et al. 1996). Left TPJ has also been implicated in verbal short-term memory (Ravizza et al. 2011). The right TPJ has been more frequently implicated in social processing and aspects of attention, including attention shifts (Shulman et al. 2007, 2009, 2010; Corbetta et al. 2008; Mars et al. 2012; Bzdok et al. 2013; Krall et al. 2015). In the present study, although left and right TPJ were submitted to connectivity clustering separately, the identified TPJ clusters and corresponding connectivity patterns were largely bilateral. We did not specifically assess lateral bias in TPJ networks across the group (Kucyi et al. 2012); however, we did find specific and distinct correlations with phonemic decoding from TPJ seeds in both the left and right hemispheres. This suggests that right hemisphere networks involved in both visual processing and attention (among other functions) may be important for reading skill, though in a manner distinct from the left hemisphere networks.

While most hypotheses regarding functional connectivity differences in patient populations center on reductions in positive connectivity, it is notable that in the present study several negative connections showed a significant relationship with reading skill. Although some studies have focused on group differences without reporting the direction of baseline connectivity (Finn et al. 2013), several recent RD studies have also observed significant differences in anticorrelation or negative connectivity in RD. Remediated readers showed more negative connectivity between left fusiform gyrus and right medial prefrontal cortex relative to typical and nonremediated dyslexic readers (Koyama et al. 2013). Several regions that are typically anticorrelated with the left IPL, including anterior cingulate, post-central gyrus, right hippocampus, and precuneus, are less anticorrelated or positively correlated in RD readers across reading and resting tasks

(Schurz et al. 2014). While interpretation of differences in negative connectivity can be more challenging, findings involving negative connectivity in RD, psychiatric (Cullen et al. 2014; Stegmayer et al. 2014), and neurodevelopmental disorders (Jung et al. 2014) suggest that variability in negative connectivity may be an important predictor of symptoms and warrants further research.

The use of a data-driven parcellation to identify functional subdivisions within the TPJ, and a well characterized and adequately sized community adult sample, are strengths of the current study; however, it is also not without limitations. The duration of the resting scan was 6 min. While this duration is not atypical (Koyama et al. 2011), some studies suggest that longer scans may provide improved convergence of intervoxel correlations (Birn et al. 2013). Participants had their eyes closed during the scan, and no physiological monitoring was conducted to ensure that they were not sleeping. After the scan session, participants were asked whether they fell asleep, and none reported doing so. However, we cannot rule out the possibility that some participants may have fallen asleep during the scan. ADHD is highly comorbid with RD in children (Semrud-Clikeman et al. 1992), and 2 participants reported a previous diagnosis of ADHD. However, clinical or subclinical symptoms of inattention were not assessed as part of this study. As noted above, it is not clear whether findings here using regression against continuous reading measures would generalize to group differences between typical readers and adults with a clear diagnosis of RD. We also note that in adult readers, it is challenging to distinguish connectivity patterns related to the core deficit of reading difficulties from patterns related to differences in experience and compensation strategies that may have been in operation for decades.

In conclusion, our findings suggest that individual variability in reading depends on connectivity within TPJ networks. Specifically, our results show overconnectivity of anterior caudate in weaker readers, suggesting that hyperactivation of dorsal striatum frequently reported in RD may be caused by overintegration with fronto-parietal attention networks. More broadly, our results support theories that reading skill depends on integration of multiple domain-general networks (Vogel et al. 2013; Fedorenko and Thompson-Schill 2014), with regions around the TPJ that have previously been implicated in reading.

Supplementary Material

Supplementary material can be found at: http://www.cercor.oxfordjournals.org/.

Funding

S.A. was supported by a studentship from the Hotchkiss Brain Institute. S.B. was supported by an NSERC Discovery Grant and the Alberta Children's Hospital Foundation (ACHF). F.H. was funded by Eunice Kennedy Shriver National Institute of Child Health and Human Development Grants K23HD054720, R01HD067254 (PI: L. Cutting, Vanderbilt U), R01HD065794 (PI: K. Pugh, Haskins Labs), P01HD001994 (PI: J. Rueckl, Haskins Labs), and the National Institute of Mental Health R01MH104438 (PI: C Wu Nordahl, UC Davis MIND Institute); the Flora Family Foundation; a University of California, San Francisco (UCSF) Catalyst Award, the UCSF Resource Allocation Program, and the Dyslexia Foundation through the Extraordinary Brain Series.

Notes

Conflict of Interest: None declared.

References

Ali N, Green DW, Kherif F, Devlin JT, Price CJ. 2010. The role of the left head of caudate in suppressing irrelevant words. J Cogn Neurosci. 22:2369–2386.

Barquero LA, Davis N, Cutting LE. 2014. Neuroimaging of reading intervention: a systematic review and activation likelihood estimate meta-analysis. PLoS ONE. 9:e83668.

Binder JR, Desai RH, Graves WW, Conant LL. 2009. Where is the semantic system? A critical review and meta-analysis of 120 functional neuroimaging studies. Cereb Cortex. 19:2767–2796.

Binder JR, Frost JA, Hammeke TA, Cox RW, Rao SM, Prieto T. 1997. Human brain language areas identified by functional magnetic resonance imaging. J Neurosci. 17:353–362.

Birn RM, Molloy EK, Patriat R, Parker T, Meier TB, Kirk GR, Nair VA, Meyerand ME, Prabhakaran V. 2013. The effect of scan length on the reliability of resting-state fMRI connectivity estimates. Neuroimage. 83:550–558.

Black JM, Tanaka H, Stanley L, Nagamine M, Zakerani N, Thurston A, Kesler S, Hulme C, Lyytinen H, Glover GH, et al. 2012. Maternal history of reading difficulty is associated with reduced language-related gray matter in beginning readers. Neuroimage. 59:3021–3032.

Boets B. 2014. Dyslexia: reconciling controversies within an integrative developmental perspective. Trends Cogn Sci (Regul Ed). 18:501–503.

Boets B, Op de Beeck HP, Vandermosten M, Scott SK, Gillebert CR, Mantini D, Bulthé J, Sunaert S, Wouters J, Ghesquière P. 2013. Intact but less accessible phonetic representations in adults with dyslexia. Science. 342:1251–1254.

Bogon J, Finke K, Stenneken P. 2014. TVA-based assessment of visual attentional functions in developmental dyslexia. Front Psychol. 5:1172.

Bradley L, Bryant PE. 1978. Difficulties in auditory organisation as a possible cause of reading backwardness. Nature. 271:746–747.

Bray S, Arnold AE, Levy RM, Iaria G. 2015. Spatial and temporal functional connectivity changes between resting and attentive states. Hum Brain Mapp. 36:549–565.

Bray S, Hoeft F, Hong DS, Reiss AL. 2013. Aberrant functional network recruitment of posterior parietal cortex in turner syndrome. Hum Brain Mapp. 34:3117–3128.

Brunswick N, McCrory E, Price CJ, Frith CD, Frith U. 1999. Explicit and implicit processing of words and pseudowords by adult developmental dyslexics: a search for Wernicke's Wortschatz? Brain. 122(Pt 10):1901–1917.

Bzdok D, Langner R, Schilbach L, Jakobs O, Roski C, Caspers S, Laird AR, Fox PT, Zilles K, Eickhoff SB. 2013. Characterization of the temporo-parietal junction by combining data-driven parcellation, complementary connectivity analyses, and functional decoding. Neuroimage. 81:381–392.

Clark KA, Helland T, Specht K, Narr KL, Manis FR, Toga AW, Hugdahl K. 2014. Neuroanatomical precursors of dyslexia identified from pre-reading through to age 11. Brain. 137:3136–3141.

Corbetta M, Patel G, Shulman GL. 2008. The reorienting system of the human brain: from environment to theory of mind. Neuron. 58:306–324.

Cullen KR, Westlund MK, Klimes-Dougan B, Mueller BA, Houri A, Eberly LE, Lim KO. 2014. Abnormal amygdala resting-state functional connectivity in adolescent depression. JAMA Psychiatry. 71:1138–1147.

Demb JB, Boynton GM, Heeger DJ. 1998. Functional magnetic resonance imaging of early visual pathways in dyslexia. J Neurosci. 18:6939–6951.

Démonet JF, Price C, Wise R, Frackowiak RS. 1994. A PET study of cognitive strategies in normal subjects during language tasks. Influence of phonetic ambiguity and sequence processing on phoneme monitoring. Brain. 117(Pt 4):671–682.

Diehl JJ, Frost SJ, Sherman G, Mencl WE, Kurian A, Molfese P, Landi N, Preston J, Soldan A, Fulbright RK, et al. 2014. Neural correlates of language and non-language visuospatial processing in adolescents with reading disability. Neuroimage. 101:653–666.

Dunn LM, Dunn LM. 1997. Peabody Picture Vocabulary Test—3. Circle Pines, MN: AGS.

Fabbro F. 2000. Introduction to language and cerebellum. J Neurolinguistics. 13:83–94.

Facoetti A, Corradi N, Ruffino M, Gori S, Zorzi M. 2010. Visual spatial attention and speech segmentation are both impaired in preschoolers at familial risk for developmental dyslexia. Dyslexia. 16:226–239.

Facoetti A, Lorusso ML, Paganoni P, Cattaneo C, Galli R, Mascetti GG. 2003. The time course of attentional focusing in dyslexic and normally reading children. Brain Cogn. 53:181–184.

Facoetti A, Molteni M. 2001. The gradient of visual attention in developmental dyslexia. Neuropsychologia. 39:352–357.

Facoetti A, Paganoni P, Turatto M, Marzola V, Mascetti GG. 2000. Visual-spatial attention in developmental dyslexia. Cortex. 36:109–123.

Facoetti A, Trussardi AN, Ruffino M, Lorusso ML, Cattaneo C, Galli R, Molteni M, Zorzi M. 2010. Multisensory spatial attention deficits are predictive of phonological decoding skills in developmental dyslexia. J Cogn Neurosci. 22:1011–1025.

Facoetti A, Zorzi M, Cestnick L, Lorusso ML, Molteni M, Paganoni P, Umilta C, Mascetti GG. 2006. The relationship between visuo-spatial attention and nonword reading in developmental dyslexia. Cogn Neuropsychol. 23:841–855.

Fan Q, Anderson AW, Davis N, Cutting LE. 2014. Structural connectivity patterns associated with the putative visual word form area and children's reading ability. Brain Res. 1586:118–129.

Fedorenko E, Thompson-Schill SL. 2014. Reworking the language network. Trends Cogn Sci (Regul Ed). 18:120–126.

Fiez JA, Raichle ME, Balota DA, Tallal P, Petersen SE. 1996. PET activation of posterior temporal regions during auditory word presentation and verb generation. Cereb Cortex. 6:1–10.

Finn ES, Shen X, Holahan JM, Scheinost D, Lacadie C, Papademetris X, Shaywitz SE, Shaywitz BA, Constable RT. 2013. Disruption of functional networks in dyslexia: a whole-brain, data-driven analysis of connectivity. Biol Psychiatry. 76:397–404.

Fletcher JM. 2009. Dyslexia: the evolution of a scientific concept. J Int Neuropsychol Soc. 15:501–508.

Fox MD, Snyder AZ, Vincent JL, Corbetta M, Van Essen DC, Raichle ME. 2005. The human brain is intrinsically organized into dynamic, anticorrelated functional networks. Proc Natl Acad Sci USA. 102:9673–9678.

Franceschini S, Gori S, Ruffino M, Pedrolli K, Facoetti A. 2012. A causal link between visual spatial attention and reading acquisition. Curr Biol. 22:814–819.

Franceschini S, Gori S, Ruffino M, Viola S, Molteni M, Facoetti A. 2013. Action video games make dyslexic children read better. Curr Biol. 23:462–466.

Glover GH, Law CS. 2001. Spiral-in/out BOLD fMRI for increased SNR and reduced susceptibility artifacts. Magn Reson Med. 46:515–522.

Gori S, Mascheretti S, Giora E, Ronconi L, Ruffino M, Quadrelli E, Facoetti A, Marino C. 2015. The DCDC2 intron 2 deletion impairs illusory motion perception unveiling the selective role of magnocellular-dorsal stream in reading (dis)ability. Cereb Cortex. 25:1685–1695.

Hampson M, Tokoglu F, Sun Z, Schafer RJ, Skudlarski P, Gore JC, Constable RT. 2006. Connectivity-behavior analysis reveals that functional connectivity between left BA39 and Broca's area varies with reading ability. Neuroimage. 31:513–519.

Hari R, Renvall H, Tanskanen T. 2001. Left minineglect in dyslexic adults. Brain. 124:1373–1380.

Hoeft F, McCandliss BD, Black JM, Gantman A, Zakerani N, Hulme C, Lyytinen H, Whitfield-Gabrieli S, Glover GH, Reiss AL, et al. 2011. Neural systems predicting long-term outcome in dyslexia. Proc Natl Acad Sci USA. 108:361–366.

Hoeft F, Meyler A, Hernandez A, Juel C, Taylor-Hill H, Martindale JL, McMillon G, Kolchugina G, Black JM, Faizi A, et al. 2007. Functional and morphometric brain dissociation between dyslexia and reading ability. Proc Natl Acad Sci USA. 104:4234–4239.

Jorm AF, Share DL, Maclean R, Matthews R. 1986. Cognitive factors at school entry predictive of specific reading retardation and general reading backwardness: a research note. J Child Psychol Psychiatry. 27:45–54.

Jung M, Kosaka H, Saito DN, Ishitobi M, Morita T, Inohara K, Asano M, Arai S, Munesue T, Tomoda A, et al. 2014. Default mode network in young male adults with autism spectrum disorder: relationship with autism spectrum traits. Mol Autism. 5:35.

Koyama MS, Di Martino A, Kelly C, Jutagir DR, Sunshine J, Schwartz SJ, Castellanos FX, Milham MP. 2013. Cortical signatures of dyslexia and remediation: an intrinsic functional connectivity approach. PLoS ONE. 8:e55454.

Koyama MS, Di Martino A, Zuo XN, Kelly C, Mennes M, Jutagir DR, Castellanos FX, Milham MP. 2011. Resting-state functional connectivity indexes reading competence in children and adults. J Neurosci. 31:8617–8624.

Krafnick AJ, Flowers DL, Luetje MM, Napoliello EM, Eden GF. 2014. An investigation into the origin of anatomical differences in dyslexia. J Neurosci. 34:901–908.

Krall SC, Rottschy C, Oberwelland E, Bzdok D, Fox PT, Eickhoff SB, Fink GR, Konrad K. 2015. The role of the right temporoparietal junction in attention and social interaction as revealed by ALE meta-analysis. Brain Struct Funct. 220:587–604.

Kronbichler M, Hutzler F, Staffen W, Mair A, Ladurner G, Wimmer H. 2006. Evidence for a dysfunction of left posterior reading areas in German dyslexic readers. Neuropsychologia. 44:1822–1832.

Kucyi A, Hodaie M, Davis KD. 2012. Lateralization in intrinsic functional connectivity of the temporoparietal junction with salience- and attention-related brain networks. J Neurophysiol. 108:3382–3392.

Lee H, Devlin JT, Shakeshaft C, Stewart LH, Brennan A, Glensman J, Pitcher K, Crinion J, Mechelli A, Frackowiak RS, et al. 2007. Anatomical traces of vocabulary acquisition in the adolescent brain. J Neurosci. 27:1184–1189.

Lefly DL, Pennington BF. 2000. Reliability and validity of the adult reading history questionnaire. J Learn Disabil. 33: 286–296.

Liddle EB, Jackson GM, Rorden C, Jackson SR. 2009. Lateralized temporal order judgement in dyslexia. Neuropsychologia. 47:3244–3254.

Linkersdörfer J, Lonnemann J, Lindberg S, Hasselhorn M, Fiebach CJ. 2012. Grey matter alterations co-localize with functional abnormalities in developmental dyslexia: an ALE meta-analysis. PLoS ONE. 7:e43122.

Maisog JM, Einbinder ER, Flowers DL, Turkeltaub PE, Eden GF. 2008. A meta-analysis of functional neuroimaging studies of dyslexia. Ann NY Acad Sci. 1145:237–259.

Maldjian JA, Laurienti PJ, Kraft RA, Burdette JH. 2003. An automated method for neuroanatomic and cytoarchitectonic atlas-based interrogation of fMRI data sets. Neuroimage. 19:1233–1239.

Mars RB, Jbabdi S, Sallet J, O'Reilly JX, Croxson PL, Olivier E, Noonan MP, Bergmann C, Mitchell AS, Baxter MG, et al. 2011. Diffusion-weighted imaging tractography-based parcellation of the human parietal cortex and comparison with human and macaque resting-state functional connectivity. J Neurosci. 31:4087–4100.

Mars RB, Sallet J, Schüffelgen U, Jbabdi S, Toni I, Rushworth MF. 2012. Connectivity-based subdivisions of the human right "temporoparietal junction area": evidence for different areas participating in different cortical networks. Cereb Cortex. 22:1894–1903.

Maurer U, Bucher K, Brem S, Brandeis D. 2003. Altered responses to tone and phoneme mismatch in kindergartners at familial dyslexia risk. Neuroreport. 14:2245–2250.

McCandliss BD, Cohen L, Dehaene S. 2003. The visual word form area: expertise for reading in the fusiform gyrus. Trends Cogn Sci (Regul Ed). 7:293–299.

McDermott KB, Petersen SE, Watson JM, Ojemann JG. 2003. A procedure for identifying regions preferentially activated by attention to semantic and phonological relations using functional magnetic resonance imaging. Neuropsychologia. 41:293–303.

McGrew KS, Woodcock RW. 2001. Technical Manual, Woodcock-Johnson III. Itasca, IL: Riverside.

Milne RD, Syngeniotis A, Jackson G, Corballis MC. 2002. Mixed lateralization of phonological assembly in developmental dyslexia. Neurocase. 8:205–209.

Nelson SM, Cohen AL, Power JD, Wig GS, Miezin FM, Wheeler ME, Velanova K, Donaldson DI, Phillips JS, Schlaggar BL, et al. 2010. A parcellation scheme for human left lateral parietal cortex. Neuron. 67:156–170.

Nicolson RI, Fawcett AJ, Brookes RL, Needle J. 2010. Procedural learning and dyslexia. Dyslexia. 16:194–212.

Ojemann G, Ojemann J, Lettich E, Berger M. 1989. Cortical language localization in left, dominant hemisphere. An electrical stimulation mapping investigation in 117 patients. J Neurosurg. 71:316–326.

Power JD, Cohen AL, Nelson SM, Wig GS, Barnes KA, Church JA, Vogel AC, Laumann TO, Miezin FM, Schlaggar BL, et al. 2011. Functional network organization of the human brain. Neuron. 72:665–678.

Power JD, Schlaggar BL, Lessov-Schlaggar CN, Petersen SE. 2013. Evidence for hubs in human functional brain networks. Neuron. 79:798–813.

Price CJ. 2012. A review and synthesis of the first 20 years of PET and fMRI studies of heard speech, spoken language and reading. Neuroimage. 62:816–847.

Ravizza SM, Delgado MR, Chein JM, Becker JT, Fiez JA. 2004. Functional dissociations within the inferior parietal cortex in verbal working memory. Neuroimage. 22:562–573.

Ravizza SM, Hazeltine E, Ruiz S, Zhu DC. 2011. Left TPJ activity in verbal working memory: implications for storage- and sensory-specific models of short term memory. Neuroimage. 55:1836–1846.

Richlan F, Kronbichler M, Wimmer H. 2009. Functional abnormalities in the dyslexic brain: a quantitative meta-analysis of neuroimaging studies. Hum Brain Mapp. 30:3299–3308.

Richlan F, Kronbichler M, Wimmer H. 2011. Meta-analyzing brain dysfunctions in dyslexic children and adults. Neuroimage. 56:1735–1742.

Richlan F, Kronbichler M, Wimmer H. 2013. Structural abnormalities in the dyslexic brain: a meta-analysis of voxel-based morphometry studies. Hum Brain Mapp. 34:3055–3065.

Rizzolatti G, Matelli M. 2003. Two different streams form the dorsal visual system: anatomy and functions. Exp Brain Res. 153:146–157.

Rodgers B. 1983. The identification and prevalence of specific reading retardation. Br J Educ Psychol. 53(Pt 3):369–373.

Ronconi L, Basso D, Gori S, Facoetti A. 2014. TMS on right frontal eye fields induces an inflexible focus of attention. Cereb Cortex. 24:396–402.

Schurz M, Wimmer H, Richlan F, Ludersdorfer P, Klackl J, Kronbichler M. 2014. Resting-state and task-based functional brain connectivity in developmental dyslexia. Cereb Cortex. doi:10.1093/cercor/bhu184 [Epub ahead of print].

Seeley WW, Menon V, Schatzberg AF, Keller J, Glover GH, Kenna H, Reiss AL, Greicius MD. 2007. Dissociable intrinsic connectivity networks for salience processing and executive control. J Neurosci. 27:2349–2356.

Semrud-Clikeman M, Biederman J, Sprich-Buckminster S, Lehman BK, Faraone SV, Norman D. 1992. Comorbidity between ADDH and learning disability: a review and report in a clinically referred sample. J Am Acad Child Adolesc Psychiatry. 31:439–448.

Shaywitz BA, Shaywitz SE, Pugh KR, Mencl WE, Fulbright RK, Skudlarski P, Constable RT, Marchione KE, Fletcher JM, Lyon GR, et al. 2002. Disruption of posterior brain systems for reading in children with developmental dyslexia. Biol Psychiatry. 52:101–110.

Shaywitz SE, Escobar MD, Shaywitz BA, Fletcher JM, Makuch R. 1992. Evidence that dyslexia may represent the lower tail of a normal distribution of reading ability. N Engl J Med. 326:145–150.

Shaywitz SE, Shaywitz BA. 2008. Paying attention to reading: the neurobiology of reading and dyslexia. Dev Psychopathol. 20:1329–1349.

Shaywitz SE, Shaywitz BA, Fulbright RK, Skudlarski P, Mencl WE, Constable RT, Pugh KR, Holahan JM, Marchione KE, Fletcher JM, et al. 2003. Neural systems for compensation and persistence: young adult outcome of childhood reading disability. Biol Psychiatry. 54:25–33.

Shaywitz SE, Shaywitz BA, Pugh KR, Fulbright RK, Constable RT, Mencl WE, Shankweiler DP, Liberman AM, Skudlarski P, Fletcher JM, et al. 1998. Functional disruption in the organization of the brain for reading in dyslexia. Proc Natl Acad Sci USA. 95:2636–2641.

Shulman GL, Astafiev SV, Franke D, Pope DL, Snyder AZ, McAvoy MP, Corbetta M. 2009. Interaction of stimulus-driven reorienting and expectation in ventral and dorsal frontoparietal and basal ganglia-cortical networks. J Neurosci. 29:4392–4407.

Shulman GL, Astafiev SV, McAvoy MP, d'Avossa G, Corbetta M. 2007. Right TPJ deactivation during visual search: functional significance and support for a filter hypothesis. Cereb Cortex. 17:2625–2633.

Shulman GL, Pope DL, Astafiev SV, McAvoy MP, Snyder AZ, Corbetta M. 2010. Right hemisphere dominance during spatial selective attention and target detection occurs outside the dorsal frontoparietal network. J Neurosci. 30:3640–3651.

Sireteanu R, Goertz R, Bachert I, Wandert T. 2005. Children with developmental dyslexia show a left visual "minineglect". Vision Res. 45:3075–3082.

Snowling M. 1998. Dyslexia as a phonological deficit: evidence and implications. Child Psych and Psychiatry Rev. 3:4–11.

Sridharan D, Levitin DJ, Menon V. 2008. A critical role for the right fronto-insular cortex in switching between central-executive and default-mode networks. Proc Natl Acad Sci USA. 105: 12569–12574.

Stegmayer K, Usher J, Trost S, Henseler I, Tost H, Rietschel M, Falkai P, Gruber O. 2014. Disturbed cortico-amygdalar functional connectivity as pathophysiological correlate of working memory deficits in bipolar affective disorder. Eur Arch Psychiatry Clin Neurosci. 265:303–311.

Stevenson J. 1988. Which aspects of reading ability show a "hump"in their distribution? Appl Cognitive Psych. 2:77–85.

Torgesen JK, Wagner R, Rashotte C. 1999. TOWRE–2 Test of Word Reading Efficiency. Austin (TX): Pro-Ed.

Turkeltaub PE, Gareau L, Flowers DL, Zeffiro TA, Eden GF. 2003. Development of neural mechanisms for reading. Nat Neurosci. 6:767–773.

Tzourio-Mazoyer N, Landeau B, Papathanassiou D, Crivello F, Etard O, Delcroix N, Mazoyer B, Joliot M. 2002. Automated anatomical labeling of activations in SPM using a macroscopic anatomical parcellation of the MNI MRI single-subject brain. Neuroimage. 15:273–289.

Valdois S, Bosse ML, Tainturier MJ. 2004. The cognitive deficits responsible for developmental dyslexia: review of evidence for a selective visual attentional disorder. Dyslexia. 10: 339–363.

Vandenberghe R, Price C, Wise R, Josephs O, Frackowiak RS. 1996. Functional anatomy of a common semantic system for words and pictures. Nature. 383:254–256.

van der Mark S, Klaver P, Bucher K, Maurer U, Schulz E, Brem S, Martin E, Brandeis D. 2011. The left occipitotemporal system in reading: disruption of focal fMRI connectivity to left inferior frontal and inferior parietal language areas in children with dyslexia. Neuroimage. 54:2426–2436.

Vigneau M, Beaucousin V, Hervé PY, Duffau H, Crivello F, Houdé O, Mazoyer B, Tzourio-Mazoyer N. 2006. Meta-analyzing left hemisphere language areas: phonology, semantics, and sentence processing. Neuroimage. 30:1414–1432.

Vogel AC, Church JA, Power JD, Miezin FM, Petersen SE, Schlaggar BL. 2013. Functional network architecture of reading-related regions across development. Brain Lang. 125:231–243.

Vogel AC, Miezin FM, Petersen SE, Schlaggar BL. 2012. The putative visual word form area is functionally connected to the dorsal attention network. Cereb Cortex. 22:537–549.

Wagner RK, Torgesen JK. 1987. The nature of phonological processing and its causal role in the acquisition of reading skills. Psychol Bull. 101:192–212.

Wechsler D. 1999. Wechsler Abbreviated Scale of Intelligence (WASI). San Antonio (TX): The Psychological Corporation.

Wolf M, Denckla MB. 2005. Rapid automatized naming and rapid alternating stimulus tests. Austin (TX): Pro-Ed.

Woodcock RW. 1987. Woodcock Reading Mastery Tests, Revised. Circle Pines (MI): American Guidance Service.